MULTIFUNCTIONAL POLYMER COMPOSITES REINFORCED WITH DISCONTINUOUS CARBON FIBERS FOR THERMAL ENERGY STORAGE

Giulia Fredi[1], Andrea Dorigato[1], Luca Fambri[1] and Alessandro Pegoretti[1]

[1]University of Trento, Department of Industrial Engineering, Via Sommarive 9 - 38123 Trento, Italy
giulia.fredi@unitn.it; andrea.dorigato@unitn.it; luca.fambri@unitn.it; alessandro.pegoretti@unitn.it

Keywords: multifunctional composites, discontinuous carbon fibers, thermoplastic composites, thermal energy storage, phase change materials.

Abstract

In this work, multifunctional semistructural composites for thermal energy storage (TES) were produced by adding discontinuous carbon fibers and a microencapsulated paraffin in a thermoplastic (polyamide 12, PA12) or thermosetting (epoxy) matrix. The microstructural, thermal and mechanical properties of the resulting composites were investigated. SEM images demonstrated the achievement of a good microfiller dispersion and an acceptable fiber-matrix adhesion in both cases. DSC tests revealed that, for both matrices, the melting enthalpy increased with the capsules amount, but the TES capability of the PA12 composites was limited by the partial capsules breakage and the consequent molten paraffin leakage during melt compounding, while no enthalpy decrease was detected for epoxy composites. The introduction of microcapsules in both matrices determined a decrease of the elastic modulus, stress at yield and deformation at break, even when a carbon reinforcement was present, probably because of the limited interfacial adhesion between the matrix and the microcapsules.

1. Introduction

Thermal energy storage (TES) can be described as the storage of heat for later uses; this technology helps in bringing together the energy availability and demand when they are far in time and space, and provides beneficial effects on thermal management processes [1]. TES systems are currently employed in many applications, such as in power generation systems and in the buildings industry, fields where there is considerable need for thermal energy, which is subjected to noticeable daily and seasonal variations. Thermal energy can be stored and released as sensible, thermochemical or latent heat. Storing latent heat with phase change materials (PCMs) is advantageous, as PCMs can accumulate a large amount of thermal energy per unit mass, at a nearly constant temperature, with a low volume change [2]. Oligomeric/polymeric PCMs, such as paraffin waxes, are the most diffused materials for TES, due to their high specific phase change enthalpy, tailorable working temperature, low density and cheapness. These materials need confinement to avoid leakage above the melting temperature. One of the ways to address this issue is the encapsulation of the PCMs in organic or inorganic micro/nano shells, which additionally act as a protective barrier against the external environment and increase the thermal stability of the PCM [3].

In some fields, weight and volume savings are a crucial point, and it would be beneficial to have a multifunctional structure that also contributes to the thermal management, to avoid the addition of extra weight [4]. Examples of materials that could be usefully employed in these cases are lightweight multifunctional polymer-matrix composites performing TES functions and a structural/semi structural role. For instance, our group developed a multifunctional epoxy/carbon fiber composites containing paraffin wax shape stabilized with carbon nanotubes (CNTs) [5, 6] and a glass/polyamide thermoplastic laminate containing a commercial microencapsulated paraffin [7]. However, the field of multifunctional short-fiber composites with TES capability is still largely unexplored, even though these materials would have great potential for thermal management applications in fields like automotive or portable electronics. The aim of this work is to produce and characterize multifunctional composites with discontinuous carbon fibers and paraffin microcapsules (MC) with a working temperature range of 40-50 °C. Two matrices have been considered; a thermoplastic matrix (i.e. polyamide 12 (PA12)) and a thermosetting matrix (i.e. epoxy resin (EP)).

2. Materials and method

2.1 Materials

Polymer granules of Rilsan® PA12 (Arkema, Lyon, France), were utilized as a polymer matrix (melting temperature 174 °C). The epoxy base Elan-tech® EC157 and the hardener Elan-tech® W342 were provided by Elantas Europe Srl. To evaluate the effect of the fiber length on the thermo-mechanical behaviour of the prepared composites, discontinuous carbon fibers with two different lengths were considered; Zoltek Panex® 35 milled carbon fibers (diameter = 7.2 µm, length of 100 µm), and Zoltek PX® 35 chopped carbon fibers (diameter = 7.2 µm, length of 6 mm). The microencapsulated PCM was the Microtek MPCM43D (Microtek Laboratories Inc.), made of a paraffinic core with a melting temperature of 43 °C, and a stable melamine-formaldehyde shell. These microcapsules were characterized by a mean diameter of 17-20 µm, and the melting enthalpy declared by the producer was 190-200 J/g. All the materials were used as received.

2.2 Production and characterization of thermoplastic PA12/CF/MC composites

PA12 granules, the reinforcing fibers and the PCM were compounded in a Thermo Haake Rheomix® 600 internal mixer at 190 °C and 40 rpm for 6 min. The resulting compounds were molded through a Carver hot-plate press at 190 °C for 10 min under an applied pressure of 1.75 MPa. Samples were designated as PA12-cap**x**-CFL/CFS**y**, where “cap” indicates the microcapsules, **x** the capsules weight fraction in the matrix, CFL and CFS the long and short carbon fibers, respectively, and **y** the CF weight fraction. Scanning electron microscopy (SEM) images of the cryofracture surfaces were acquired through a Carl Zeiss AG-SUPRA 40 microscope, after Pt-Pd sputtering. Differential scanning calorimetry (DSC) was performed with a Mettler DSC30 machine under a N_2 flow of 150 ml/min, in a temperature range between -20 °C and 240 °C, at a heating/cooling rate of 10 °C/min. Thermogravimetric analysis (TGA) was carried out by using a Mettler TG50 machine under a nitrogen flow of 200 ml/min, up to 700 °C, at a heating rate of 10 °C/min. Vicat tests were performed at a heating rate of 120 °C/h and under an applied load of 10 N. Quasi-static tensile tests were performed with a universal testing machine Instron 4502 on 1BA specimens (UNI EN ISO 527-2). For each composition, five specimens were tested at 0.25 mm/min for the measurement of the elastic modulus, using a resistance extensometer Instron 2620 with a gauge length of 12.5 mm. Five additional specimens were tested until failure, at a crosshead speed of 10 mm/min. Dynamic rheological tests have been performed by Haake Mars III DSR, under parallel plate geometry, with a maximum shear strain of 1% at 190°C. Laser flash analysis (LFA) was performed to measure the specific heat and the thermal conductivity and diffusivity, using a Netzsch LFA 447. Measurements were performed on specimens of 12.7x12.7 mm^2, tested at three temperatures (20, 40 and 60 °C).

2.3 Production and characterization of thermosetting EP/CF/MC composites

The epoxy base and the hardener were mixed at a constant ratio of 100:30 and mechanically stirred with the CF and MC at different relative concentrations at 200 rpm for 5 min. The mixtures were degassed under vacuum and poured in silicone molds. The samples were cured at ambient temperature for 24 hours, and post-cured for 10 h at 100 °C. The samples were named EP-MC**x**-CF**y**, where **x** is the weight fraction of MC in the matrix, and **y** is the total weight fraction of CFs.

SEM, DSC and TGA tests were performed in the same way as described in Paragraph 2.2. The density of the matrices and of the composites was measured with the technique of the Archimedes balance in ethanol, through a Gibertini E42 analytical balance. A comparison with the calculated theoretical density allowed the calculation of the porosity. Three-point flexural tests were performed with an Instron 5969 universal testing machine, equipped with a 50 kN load cell, on specimens of 70x10x3 mm^3. The span length was fixed at 50 mm and the crosshead speed at 1.5 mm/min. Charpy impact tests were performed at ambient temperature according to ISO 179 with a Ceast machine equipped with a hammer having a mass of 1.18 kg a length of 23 cm, and setting an initial impact angle of 23° (impact speed = 1.0 m/s). At least five specimens of 70x10x3 mm^3 with a notch depth of 2 mm and a notch radius of 0.25 mm were tested for each composition. A span length of 62 mm was utilized.

3. Results and discussion

3.1 Results of the thermoplastic PA12/CF/MC composites

SEM images of the cryofracture surfaces of the prepared composites are reported in Fig. 1(a-c). A good fiber-matrix adhesion was obtained both with CFL and CFS, while the adhesion between microcapsules and the matrix is poorer. Some capsules are broken, which happened partly during the cryofracturing operations and partly during the processing. This phenomenon could negatively affect both the mechanical behaviour of the resulting composites, and the TES capability.

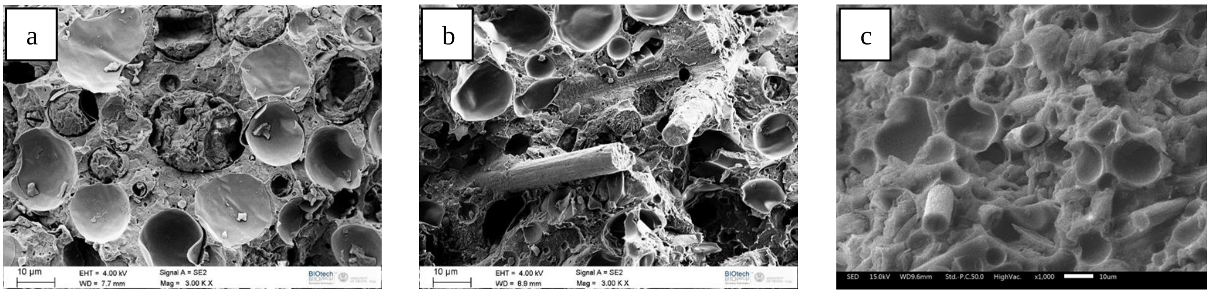

Figure 1. SEM images of (a) PA12-cap50, (b) PA12-cap50-CFL20 and (c) PA12-cap50-CFS20.

Fig. 2(a-b) report the results of the rheological test. The viscosity increases with the capsules and fibers content, but the increase is more evident with CFL than with CFS, for the same capsules content. This indicates that the shear stresses in the compounding phase are higher for mixture containing longer fibers, which could lead to a greater damage on the capsules and paraffin leakage, thus lowering the total final phase change enthalpy. The results of the DSC tests are reported in Table 1. Both the glass transition temperature (T_g) and the melting point of the polymer matrix (T'_m) are not affected by the presence of the PCM. On the other hand, the variation of the microcapsules melting temperature (T_m) is probably due to a different thermal conduction mechanism inside the testing samples. As it could be expected, the melting enthalpy (ΔH_m) increases with the PCM amount, and for the PA12-cap60 sample a ΔH_m value of 117 J/g is measured. However, the relative melting enthalpy (ΔH^R_m), i.e. the ratio between the ΔH_m values of the composites and of the neat capsules normalized by the PCM weight fraction in the composites, decreases with the capsules concentration. This could be explained by considering that the increase in viscosity due to the PCM addition determines an increase in the thermo-mechanical stress to which the capsules are subjected during the melt compounding operations, which leads to their partial breakage and the consequent paraffin leakage. This effect is even more evident with long carbon fibers. This is consistent with the results of the dynamic rheological tests. In Table 1 the most important results of TGA tests are also summarized. It is interesting to note that both the temperature associated to the onset of the degradation of the PA12 matrix (T_{onset}) and the degradation temperature (T_d), i.e. the temperature associated to the maximum mass loss rate, are not substantially affected by the presence of the carbon fibers and/or the capsules inside the material. The last column of Table 1 contains the results of the Vicat test. The Vicat softening temperature (*VST*) is slightly increased by carbon fibers addition, especially with CFL reinforcement, while microcapsules introduction does not strongly deteriorate the Vicat grade of the materials.

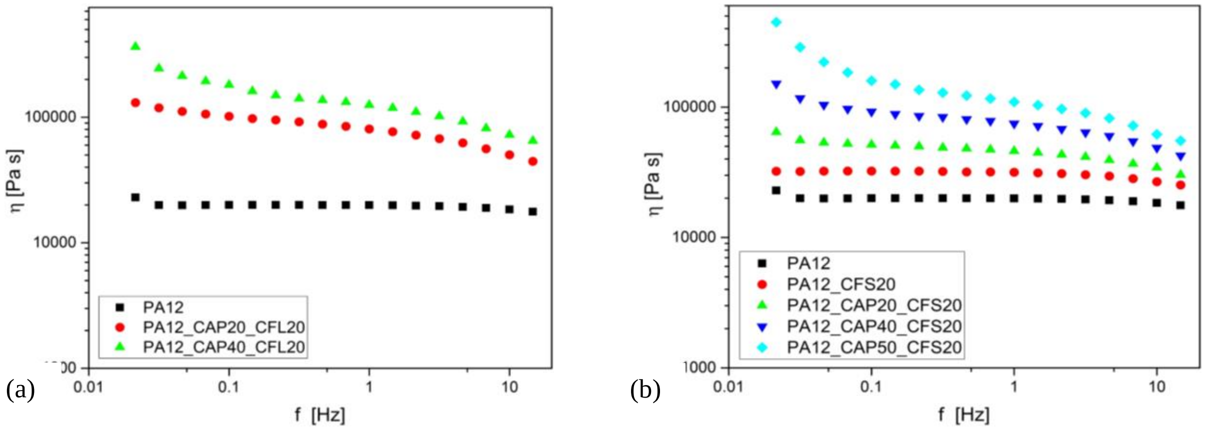

Figure 2. Results of the dynamic rheological test. (a) CFL-filled samples, (b) CFS-filled samples.

Sample	DSC					TGA		Vicat
	T_g [°C]	T_m [°C]	T'_m [°C]	ΔH_m [J/g]	ΔH^R_m [%]	T_{onset} [°C]	T_d [°C]	*VST* [°C]
cap	-	44.1		220.1	100.0	-	-	-
PA12	40.7	-	179.9	-	-	429.0	475.7	176.8 ± 0.4
PA12-cap20	-	46.2	178.7	44.5	101.1	453.9	471.5	174.7 ± 0.3
PA12-cap40	-	47.3	178.6	91.8	104.3	441.1	471.7	173.9 ± 0.4
PA12-cap50	-	49.9	180.0	100.8	91.6	444.8	468.6	174.1 ± 1.6
PA12-cap60	-	47.8	177.6	116.6	88.3	433.2	468.9	175.7 ± 1.3
PA12-CFL10	39.7	-	180.2	-	-	451.8	481.8	181.2 ± 0.4
PA12-CFL20	39.4	-	181.2	-	-	455.8	480.3	182.2 ± 0.6
PA12-CFL30	38.7	-	181.0	-	-	451.5	476.6	183.2 ± 0.4
PA12-cap20-CFL20	-	45.5	178.9	33.0	93.8	448.6	476.7	179.9 ± 0.7
PA12-cap40-CFL20	-	45.8	179.9	28.9	41.1	448.4	476.2	179.5 ± 0.4
PA12-cap50-CFL20	-	46.6	178.2	46.9	53.3	455.7	474.1	180.2 ± 0.7
PA12-cap60-CFL20	-	45.8	178.4	44.5	42.1	458.4	474.0	180.8 ± 0.6
PA12-CFS10	41.0	-	180.4	-	-	453.7	474.7	179.0 ± 0.3
PA12-CFS20	37.6	-	180.0	-	-	448.0	471.5	176.9 ± 0.3
PA12-CFS30	37.1	-	180.6	-	-	450.8	479.2	179.9 ± 0.3
PA12-cap20-CFS20	-	45	179.2	33.3	94.6	449.7	474.1	177.6 ± 0.3
PA12-cap40-CFS20	-	48.1	179.6	58.8	83.5	448.7	474.0	176.1 ± 0.6
PA12-cap50-CFS20	-	47.5	179.4	60.4	61.0	448.7	475.0	176.4 ± 0.3
PA12-cap60-CFS20	-	44.8	177.8	54.6	51.7	446.9	477.3	177.9 ± 0.6

Table 1. Main results of the thermal analysis (DSC, TGA and Vicat tests) on the prepared composites.

The results of the quasi-static tensile tests are reported in Fig. 3(a-b). The introduction of microcapsules in the PA12 matrix determines a decrease in the elastic modulus (E), of the stress at yield (σ_y) and of the deformation at break (ε_b). As expected, the introduction of carbon fibers within the material determines an increase in the stiffness and of the maximum stress, coupled with an evident reduction of the strain at break, and this effect is more evident for the samples containing the CFL reinforcement. The introduction of the microcapsules determines a deterioration of the mechanical performances also in the carbon fiber reinforced materials. As shown in the SEM images reported in Fig. 1, this effect can be explained by considering the poor interfacial adhesion between PA12 and the PCM, and further efforts will be made to tailor the surface properties of the microcapsules.

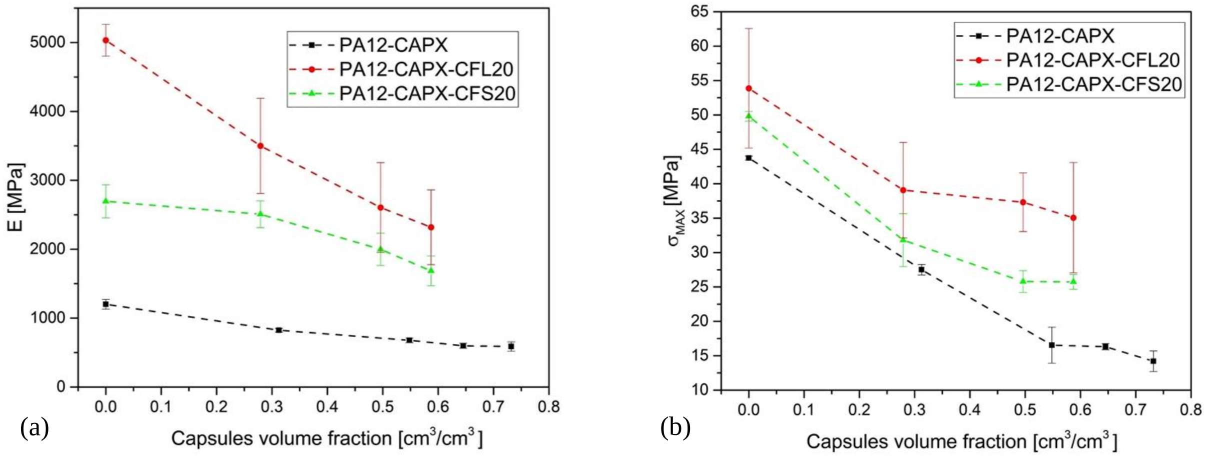

Figure 3. (a) Elastic modulus and (b) stress at break as a function of the PCM content.

3.2 Results of the thermosetting EP/CF/MC composites

Fig. 4(a-b) report the SEM images of the cryofracture surfaces of the sample EP-MC20-CF5, taken at different magnification levels. Both fillers are uniformly distributed in the matrix, and the adhesion between the epoxy and the capsule shells, even though not optimal, seems rather good and comparable to that observed between the polymer matrix and the carbonaceous reinforcement. Some capsules are broken, and since the preparation of the samples was performed at low shear mixing conditions, it is reasonable to assume that the breakage of the microcapsule shells happened during the cryofracturing process.

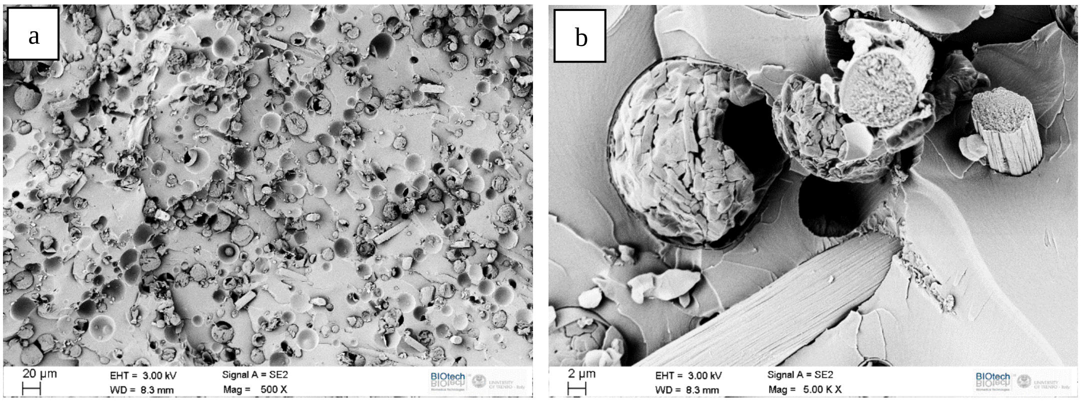

Figure 4: SEM micrographs of the cryofracture surface of EP-MC20-CF5 (a) 500x; (b) 5000x.

Table 2 summarizes the most important results obtained during DSC analysis. The values of T_g are not substantially influenced by the presence of MC and/or CF, and remain in the range 90-95 °C. The melting (T_m) and crystallization (T_c) temperatures of the MC do not significantly change when inserted in the polymer matrix, and also the presence of CF do not seem to influence the phase change temperatures in the composites. Interesting melting enthalpy (ΔH_m) values can be obtained at elevated MC concentrations. For instance, a ΔH_m value of 61 J/g can be detected for the sample EP-MC30-CF10. The ΔH^R_m values for all the samples are near 100%, which confirms that the processing and the curing operations did not cause damage to the capsules, and that the TES capability of the MC is preserved even after the incorporation in the polymer matrices. Values of ΔH^R_m above 100% are probably the result of slight inhomogeneities of the PCM distribution in the composites.

Sample	T_g (°C)	T_m (°C)	ΔH_m (J/g)	ΔH^R_m (%)	T_c (°C)	ΔH_c (J/g)
EP	94.3	-	-		-	-
MC	-	44.1	220.1	100	29.6	198.9
EP-CF10	94.7	-	-	-	-	-
EP-MC5-CF10	93.3	42.8	10.6	107.1	28.2	10.5
EP-MC15-CF10	92.8	46.5	29.5	99.3	25.8	29.1
EP-MC30-CF10	93.6	46.4	60.8	102.4	26.2	60.8
EP-MC20	95.8	47.8	47.3	107.5	24.2	46.9
EP-MC20-CF5	92.7	45.7	43.0	102.9	26.7	42.5
EP-MC20-CF10	90.0	45.9	40.2	101.5	26.3	39.6
EP-MC20-CF15	90.1	45.0	39.8	106.4	27.8	39.3

Table 2: Main results of the DSC tests on the prepared composites.

The main results of the three-point flexural test are reported in Table 3. CF addition determines an important increase in the flexural modulus (E_f) and a strong reduction in the strain at break (ε_b). For instance, for the EP-CF10 sample an increase in the elastic modulus of 65 % with respect to the neat epoxy is measured, while the ε_b is subjected to a reduction of 50 %. Also the stress at break (σ_b) slightly decreases. The observed reduction in the properties at break is not surprising, since the employed CF are unsized and the fiber-matrix adhesion is not optimal. The introduction of an increasing amount of MC determines a systematic reduction of the material stiffness, but the E_f of the EP-MCx-CF10 samples are still higher than that measured on the neat epoxy (the stiffness of the MC is probably much lower than that of a thermosetting matrix). The failure properties further decrease as the MC concentration increases. As already reported in our previous works on polymer composites with TES capability [5-7], this behaviour is probably due to the non-optimal adhesion between the PCM and the polymer matrices.

Sample	E_f (GPa)	σ_b (MPa)	ε_b (%)
EP	2.8 ± 0.5	117 ± 19	5.1 ± 0.4
EP-CF10	4.6 ± 0.2	100 ± 7	2.4 ± 0.2
EP-MC5-CF10	4.1 ± 0.3	93 ± 2	2.5 ± 0.3
EP-MC15-CF10	3.9 ± 0.2	77 ± 2	2.4 ± 0.1
EP-MC30-CF10	3.6 ± 0.1	60 ± 1	2.0 ± 0.1
EP-MC20	2.0 ± 0.4	52 ± 3	3.1 ± 0.2
EP-MC20-CF5	2.5 ± 0.2	53 ± 2	2.6 ± 0.3
EP-MC20-CF10	3.5 ± 0.2	60 ± 7	2.0 ± 0.2
EP-MC20-CF15	4.5 ± 0.3	72 ± 2	2.0 ± 0.1

Table 3: Main results of the three-point flexural test on the prepared composites.

The results of the Charpy impact test are reported in Table 4. The introduction of CF determines a slight decrease in the maximum force F_{max} (it should be noted that all the samples have the same dimensions) and of both E_{max} and E_{tot} values, which could be due to the not optimal fiber-matrix interfacial adhesion. It is interesting to note that the addition of an increasing concentration of MC does not lead to substantial variations of F_{max}, while both E_{max} and E_{tot} are even higher than those displayed by the EP-CF10 sample. This result can be probably explained by the plasticizing effect played by paraffin microcapsules within the material under impact conditions. On the other hand, the impact properties displayed by the EP-MC20 sample are lower than those of the neat matrix, but the addition of an increasing CF loading determines an interesting increase in the F_{max} values up to a level comparable to that of the neat epoxy, and also E_{max} and E_{tot} slightly increase.

Sample	F_{max} (N)	E_{max} (kJ/m^2)	E_{tot} (kJ/m^2)
EP	138 ± 52	3.5 ± 0.3	3.6 ± 2.3
EP-CF10	110 ± 22	1.6 ± 0.6	1.7 ± 0.6
EP-MC5-CF10	131 ± 3	2.7 ± 0.2	3.0 ± 0.5
EP-MC15-CF10	123 ± 5	2.5 ± 0.2	2.5 ± 0.2
EP-MC30-CF10	116 ± 13	1.7 ± 0.2	1.8 ± 0.1
EP-MC20	97 ± 10	1.6 ± 0.5	1.7 ± 0.5
EP-MC20-CF5	126 ± 19	2.0 ± 0.5	2.2 ± 0.4
EP-MC20-CF10	132 ± 6	1.8 ± 0.2	1.9 ± 0.1
EP-MC20-CF15	163 ± 9	2.0 ± 0.1	2.2 ± 0.1

Table 4: Results of the Charpy impact test.

4. Conclusions

This work aimed to produce and characterize multifunctional semistructural composites for thermal energy storage (TES). Thermoplastic and thermosetting composites were produced by adding different weight fractions of discontinuous carbon fibers and paraffin microcapsules in a PA12 and an epoxy matrix. The microstructural, thermal and mechanical properties of the resulting composites were investigated.

For the thermoplastic PA12-based composites, SEM micrographs revealed a good fiber-matrix adhesion, while the surface interaction between PA12 and the capsules could be improved. DSC test showed that the phase change enthalpy increased with the capsules content, but the relative enthalpies decreased. This was probably due to the breakage of some capsules and paraffin leakage in the melt compounding process, caused by the increase in the shear stresses due to the high melt viscosity. This was confirmed also by the results of the dynamic rheological tests, where the melt viscosity increased with an increase in the capsules content, and this effect was more evident with the longer fibers. Thus, the higher phase change enthalpies were reached in the samples with the short fibers (CFS). For the mechanical properties, the stiffness and strength of the composites decreased with an increase in the weight fraction of capsules, while they increased with the fiber content, which was more evident with the long carbon fibers, as expected.

For the thermosetting epoxy-based composites, SEM micrographs highlighted a good filler distribution, and the filler-matrix adhesion could be improved for both fillers. Also in this case, the phase change enthalpy increased with the PCM content, but for these materials the processing condition did not determine a sensible breakage of capsules, and the relative melting enthalpies are close to 100 % for all the compositions. Three-point flexural test revealed a decrease in mechanical properties as the PCM content increases, while the fibers positively contributed to increase the elastic modulus and the stress at break.

This work demonstrated the feasibility of multifunctional semistructural TES composites reinforced with discontinuous fibers. Further studies will be focused on optimizing the processing parameters to limit the capsules damage and increase the relative phase change enthalpy, and on improving the filler-matrix adhesion to obtain composites with better mechanical properties.

Acknowledgments

Mr. Nicolò Artuso is gratefully acknowledged for his support to the experimental activity.

References

[1] K. Pielichowska and K. Pielichowski, "Phase change materials for thermal energy storage", *Progress in materials science,* vol. 65, pp. 67-123, 2014.
[2] S. M. Hasnain, "Review on sustainable thermal energy storage technologies, Part I: heat storage materials and techniques", *Energy Conversion and Management,* vol. 39, pp. 1127-1138, 1998.
[3] T. Khadiran, M. Z. Hussein, Z. Zainal, and R. Rusli, "Encapsulation techniques for organic phase change materials as thermal energy storage medium: A review", *Solar Energy Materials and Solar Cells,* vol. 143, pp. 78-98, Dec 2015.
[4] S. Yoo, E. Kandare, R. Shanks, M. A. Al-Maadeed, and A. Afaghi Khatibi, "Thermophysical Properties of Multifunctional Glass Fibre Reinforced Polymer Composites Incorporating Phase Change Materials", *Thermochimica Acta,* vol. 642, pp. 25-31, 2016.
[5] G. Fredi, A. Dorigato, L. Fambri, and A. Pegoretti, "Wax Confinement with Carbon Nanotubes for Phase Changing Epoxy Blends", *Polymers,* vol. 9, p. 405, 2017.
[6] G. Fredi, A. Dorigato, L. Fambri, and A. Pegoretti, "Multifunctional epoxy/carbon fiber laminates for thermal energy storage and release", *Composites Science and Technology,* vol. 158, pp. 101-111, 2018.
[7] G. Fredi, A. Dorigato, and A. Pegoretti, "Multifunctional glass fiber/polyamide composites with thermal energy storage/release capability", *eXPRESS polymer letters,* vol. 12, pp. 349-364, 2018.